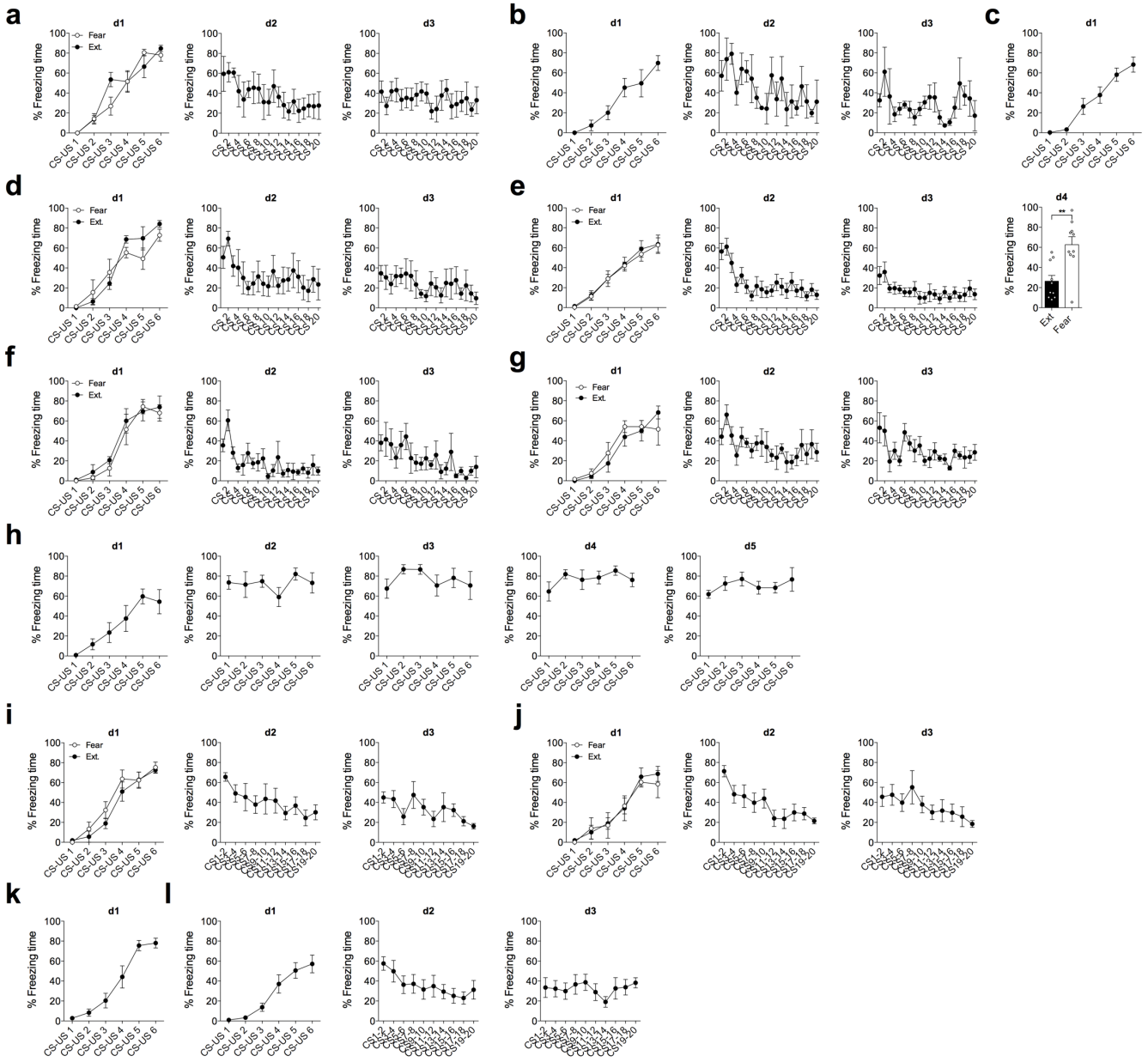

Supplementary Fig. 1. Learning curves for electrophysiological and control experiments. a, Fear conditioning and extinction learning curves from experiment in Fig. 1 (*n*=5 fear mice and *n*=5 extinction mice). **b,** Fear conditioning and extinction learning curves from experiment in Extended Data Fig. 3 (*n*=7 fear mice and *n*=3 extinction mice). **c,** Fear conditioning learning curve from experiments in Fig. 2 (*n*=14 fear mice). **d,** Fear conditioning and extinction learning curves from experiment in Fig. 3 (*n*=5 fear mice and *n*=5 extinction mice). **e,** Comparison of fear recall on day 4 (d4) from mice left in their home cage (Fear) compared to mice that have undergone extinction training (Ext) (*n*=10 mice per group; two-tailed unpaired t-test, $t_{(18)}$=3.699, *P*=0.0016). **f,** Fear conditioning and extinction learning curves from experiment in Fig. 4 (*n*=4 fear mice and n=4 extinction mice). **g,** Fear conditioning and extinction learning curves from experiment in Extended Data Fig. 4 (*n*=5 fear mice and *n*=5 extinction mice). **h,** Learning curves of 5 days of fear conditioned overtraining from experiments in Supplementary Fig. 4

(*n*=6 fear mice). **i,** Fear conditioning and extinction learning curves from experiment in Extended Data Fig. 5 (*n*=6 fear mice and *n*=5 extinction mice). **j,** Fear conditioning and extinction learning curves from experiment in Supplementary Fig. 5 (*n*=4 fear mice and *n*=5 extinction mice). **k,** Fear conditioning learning curve from experiment in Supplementary Fig. 6c-f (*n*=10 fear mice). **l,** Fear conditioning and extinction learning curves from experiment in Supplementary Fig. 6g-j (*n*=8 extinction mice). Learning curves are presented as mean ± S.E.M., and bar graphs are presented as mean + S.E.M. ***P*<0.01.

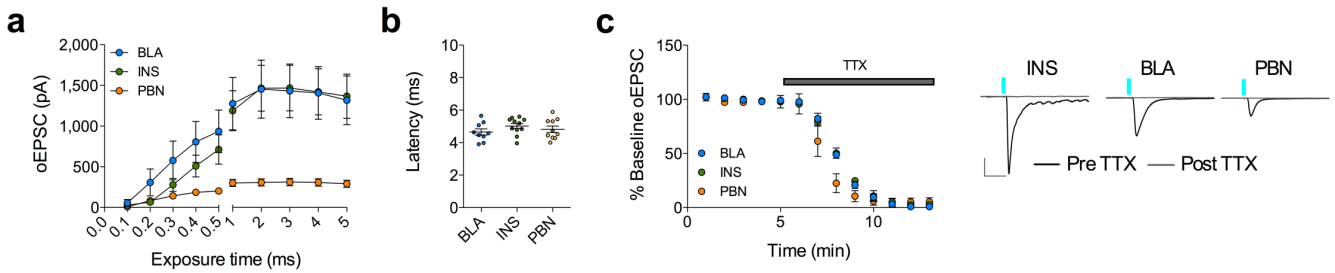

Supplementary Fig. 2. CRF+ neurons in the CeL receive greater top-down excitatory input strength relative to bottom-up input. a, Input-output oEPSC exposure curve for BLA (*n*=9 cells, 3mice), INS (*n*=11 cells, 5 mice), and PBN (*n*=10 cells, 6 mice) inputs onto CRF+ neurons in the CeL. **b,** Latency of oEPSCs from the BLA (*n*=9 cells, 3mice), INS (*n*=11 cells, 5 mice), and PBN (*n*=10 cells, 6 mice) inputs to the CeL at maximal stimulation parameters. **c,** Left: Summary data from bath application of TTX while recording oEPSC amplitude of BLA (*n*=3 cells, 1 mouse) INS (*n*=2 cells, 1 mouse), or PBN (*n*=4 cells, 2 mice) input onto CRF+ neurons in the CeL. Right: traces of INS, BLA, and PBN oEPSCs before and after TTX application (scale bar 20ms, 500pA). Current amplitude and percent baseline amplitude are presented as mean ± S.E.M. and dot plots are presented as mean ± S.E.M.

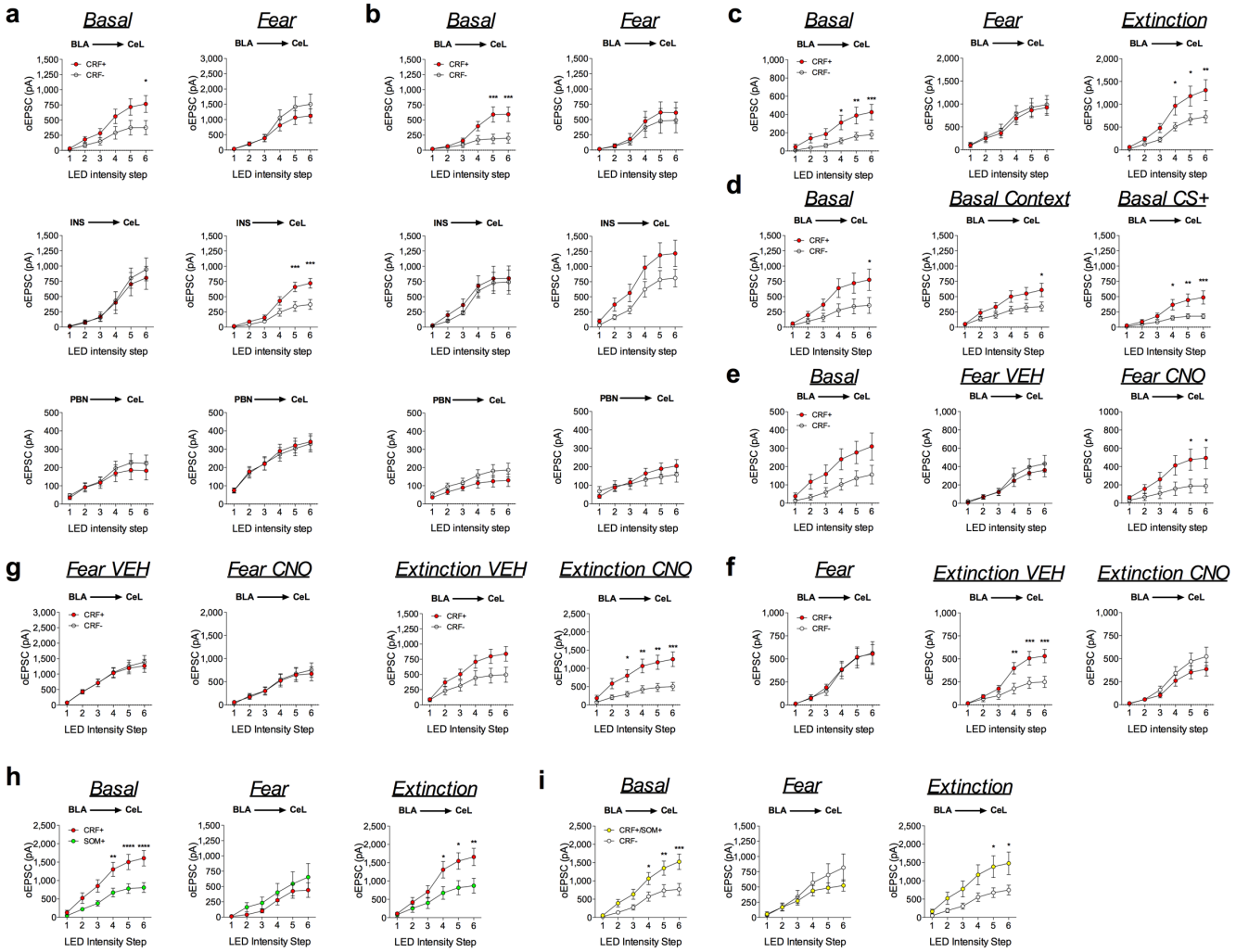

Supplementary Fig. 3. Input-output curves from dual patch-clamp recordings in the CeL. a, I/O curves of data from Fig. 2 (BLA-CeL *n*=15 basal pairs, 5 mice, *n*=14 fear pairs, 5 mice, INS-CeL *n*=15 basal pairs, 5 mice, *n*=20 fear pairs, 5 mice, PBN-CeL *n*=9 basal pairs, 5 mice, *n*=18 fear pairs, 4 mice; two-way ANOVAs, $F_{(1,168)}$=14.98, *P*=0.0002 for BLA-CeL basal group effect, and $F_{(1,228)}$=25.04, *P*<0.0001 for INS-CeL fear group effect; post-hoc Holm-Sidak's multiple comparisons, BLA-CeL basal step 6 *P*=0.0208, INS-CeL fear step 5 *P*=0.0004, step 6 *P*=0.0001). **b,** I/O curves for data from Supplementary Fig. 4 (BLA-CeL *n*=7 basal pairs, 2 mice, *n*=7 fear pairs, 2 mice, INS-CeL *n*=9 basal pairs, 2 mice, *n*=13 fear pairs, 2 mice, PBN-CeL *n*=13 basal pairs, 2 mice, *n*=11 fear pairs 2 mice; two-way ANOVAs, $F_{(1,72)}$=11.13, *P*=0.0013 for BLA-CeL basal group effect, and $F_{(1,144)}$=13.15, *P*=0.0004 for INS-CeL fear group effect; post-hoc Holm-Sidak's multiple comparisons, BLA-CeL basal step 5 *P*=0.0008, step 6 *P*=0.0009). **c,** I/O curve of data from Fig. 3 (*n*=19 basal pairs, 5 mice, *n*=18 fear pairs, 5 mice, *n*=18 extinction pairs, 5 mice; two-way ANOVAs, $F_{(1,216)}$=25.43, *P*<0.0001 for basal group effect, and $F_{(1,204)}$=19.33, *P*<0.0001 for extinction group effect; post-hoc Holm-Sidak's multiple comparisons, basal step 4 *P*=0.0360, step 5 *P*=0.0154, step 6 *P*=0.0085, extinction step 4 *P*=0.0492, step 5 *P*=0.0275, step 6 *P*=0.0091). **d,** I/O curve of data from Extended Data Fig. 3 (*n*=15 basal pairs, 4 mice, *n*=17 basal context pairs, 4 mice, and *n*=15 basal CS+ pairs, 5 mice; two-way ANOVAs, $F_{(1,168)}$=15.64, *P*=0.0001 for basal group effect, $F_{(1,192)}$=16.10, *P*<0.0001 for basal context group effect, and $F_{(1,168)}$=22.91, *P*<0.0001 for basal CS+ group effect; post-hoc Holm-Sidak's multiple comparisons, basal

step 6 P=0.0446, basal context step 6 P=0.0373, basal CS+ step 4 P=0.0310, step 5 P=0.0058, step 6 P=0.0011). **e,** I/O curve of data from Fig. 5c-f (n=17 basal pairs, 5 mice, n=20 fear VEH pairs, 5 mice, and n=19 fear CNO pairs, 5 mice; two-way ANOVAs, $F_{(1,192)}$=17.69, P<0.0001 for basal group effect, and $F_{(1,216)}$=18.38, P<0.0001 for fear CNO group effect; post-hoc Holm-Sidak's multiple comparisons, fear step 5 P=0.0368, step 6 P=0.0270). **f,** I/O curve of data from Fig. 5g-j (n=26 fear pairs, 4 mice, n=23 extinction VEH pairs, 5 mice, and n=25 extinction CNO pairs, 5 mice, two-way ANOVAs, $F_{(1,264)}$=25.08, P<0.0001 for extinction VEH group effect; post-hoc Holm-Sidak's multiple comparisons, extinction VEH step 4 P=0.0081, step 5 P=0.0010, step 6 P=0.0006). **g,** I/O curve of data from Supplementary Fig. 6c-j (n=19 fear VEH pairs, 5 mice, n=21 fear CNO pairs, 5 mice, n=17 extinction VEH pairs, 4 mice, and n=16 extinction CNO pairs, 4 mice; two-way ANOVAs, $F_{(1,192)}$=14.70, P=0002 for extinction VEH group effect, and $F_{(1,180)}$=44.76, P<0.0001 for extinction CNO group effect; post-hoc Holms-Sidak's multiple comparisons, extinction CNO step 3 P=0.0220, step 4 P=0.0030, step 5 P=0.0015, step 6 P=0.0006). **h,** I/O curve of data from Extended Data Fig. 5 (n=14 basal pairs, 5 mice, n=13 fear pairs, 6 mice, and n=12 extinction pairs, 5 mice; two-way ANOVAs, $F_{(1,156)}$=38.74, P<0.0001 for basal group effect, and $F_{(1,132)}$=19.76, P<0.0001 for extinction group effect; post-hoc Holm-Sidak's multiple comparisons, basal step 4 P=0.0066, step 5 P=0.0017, step 6 P=0.0005, extinction step 4 P=0.0406, step 5 P=0.0156, step 6 P=0.0093). **i,** I/O curve of data from Supplementary Fig. 5 (n=11 basal pairs, 4 mice, n=12 fear pairs, 4 mice, and n=14 extinction pairs, 5 mice; two-way ANOVAs, $F_{(1,120)}$=29.29, P<0.0001 for basal group effect, and $F_{(1,156)}$=22.20, P<0.0001 for extinction group effect; post-hoc Holm-Sidak's multiple comparisons, basal step 4 P=0.0411, step 5 P=0.0074, step 6 P=0.0006, extinction step 5 P=0.0319, step 6 P=0.0303). XY graphs for each intensity step are presented as mean of the absolute value for oEPSC amplitude ± S.E.M. *P<0.05, **P<0.01, ***P<0.001, ****P<0.0001.

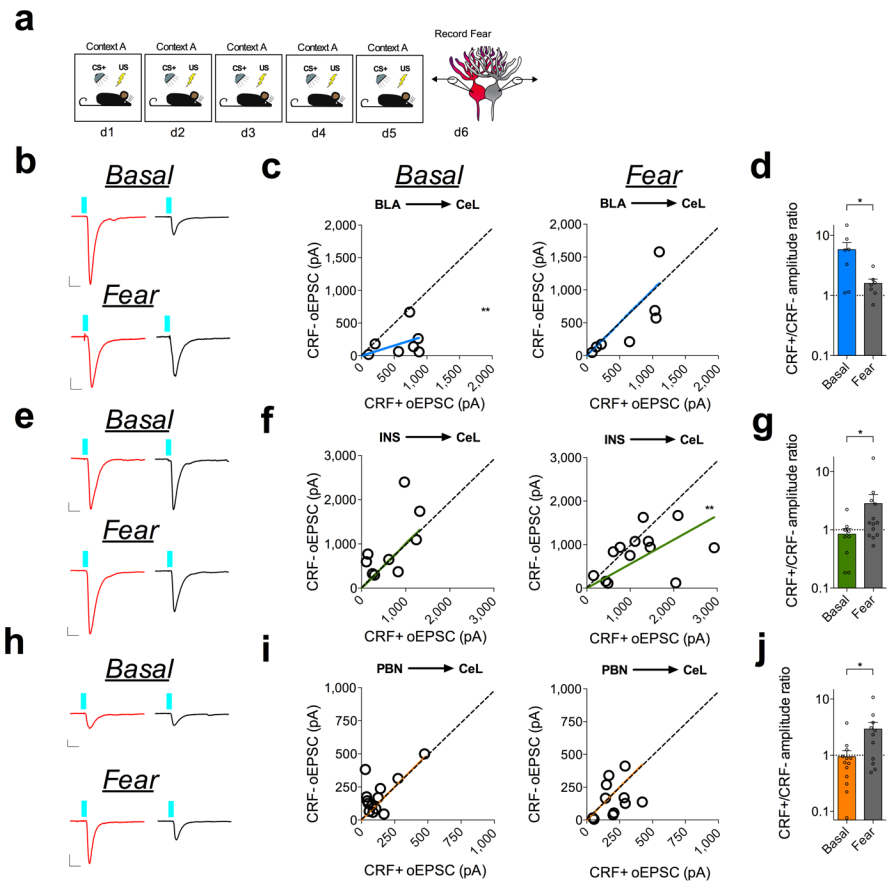

Supplementary Fig. 4. Conditioned fear overtraining remodels circuit specific input bias onto CRF+ and CRF- neurons in the CeL. a, Experimental paradigm for dual patch-clamp recordings from neighboring CRF+ and CRF- neurons in over-trained mice. Right: DIC and fluorescent overlay image of dual-patch clamp recording from CRF+ and CRF- pair. **b,** Traces of maximal oEPSC amplitude from CRF+ (red) and CRF- (black) neuronal pairs across behavioral conditions for stimulation of the BLA-CeL circuit (scale bar 10ms, 200pA for basal, and 10ms, 50pA for fear). **c,** XY graphs depicting skew-plot of maximal oEPSC amplitude from each CRF+ and CRF- neuronal pair for behavioral conditions (n=7 basal pairs, 2 mice, n=7 fear pairs, 2 mice; extra sum-of-squares F test, $F_{(1,6)}$=31.76, P=0.0013). **d,** Representation of CRF+/CRF- maximal oEPSC amplitude ratio (log scale; n=7 basal pairs, n=7 fear pairs; one-tailed Mann-Whitney test, P=0.0364). **e,** Traces of maximal oEPSC amplitude from CRF+ (red) and CRF- (black) neuronal pairs across behavioral conditions for stimulation of the INS-CeL circuit (scale bar 10ms, 50pA for basal, and 10ms, 200pA for fear). **f,** XY graphs depicting skew-plot of maximal oEPSC amplitude from each CRF+ and CRF- neuronal pair for behavioral conditions (n=9 basal pairs, 2 mice, n=13 fear pairs, 2 mice; extra sum-of-squares F test, $F_{(1,12)}$=17.88, P=0.0012). **g,** Representation of CRF+/CRF- maximal oEPSC amplitude ratio (log scale; n=9 basal pairs, n=13 fear pairs; one-tailed Mann-Whitney test, P=0.0151). **h,** Traces of maximal oEPSC amplitude from CRF+ (red) and CRF- (black) neuronal pairs across behavioral conditions for stimulation of the PBN-CeL circuit (scale bars 10ms, 50pA). **i,** XY graphs depicting skew-plot of maximal oEPSC amplitude from each CRF+ and CRF- neuronal pair for behavioral conditions (n=13 basal pairs, 2 mice, n=11 fear pairs, 2 mice; extra sum-of-squares F test, not significant, P=0.1000). **j,** Representation of CRF+/CRF- maximal oEPSC amplitude ratio (log scale; n=13 basal pairs, n=11 fear pairs; one-tailed Mann-Whitney

test, P=0.0204). XY skew-plots are presented as absolute value. Bars graphs are presented as mean + S.E.M. *P<0.05, **P<0.01.

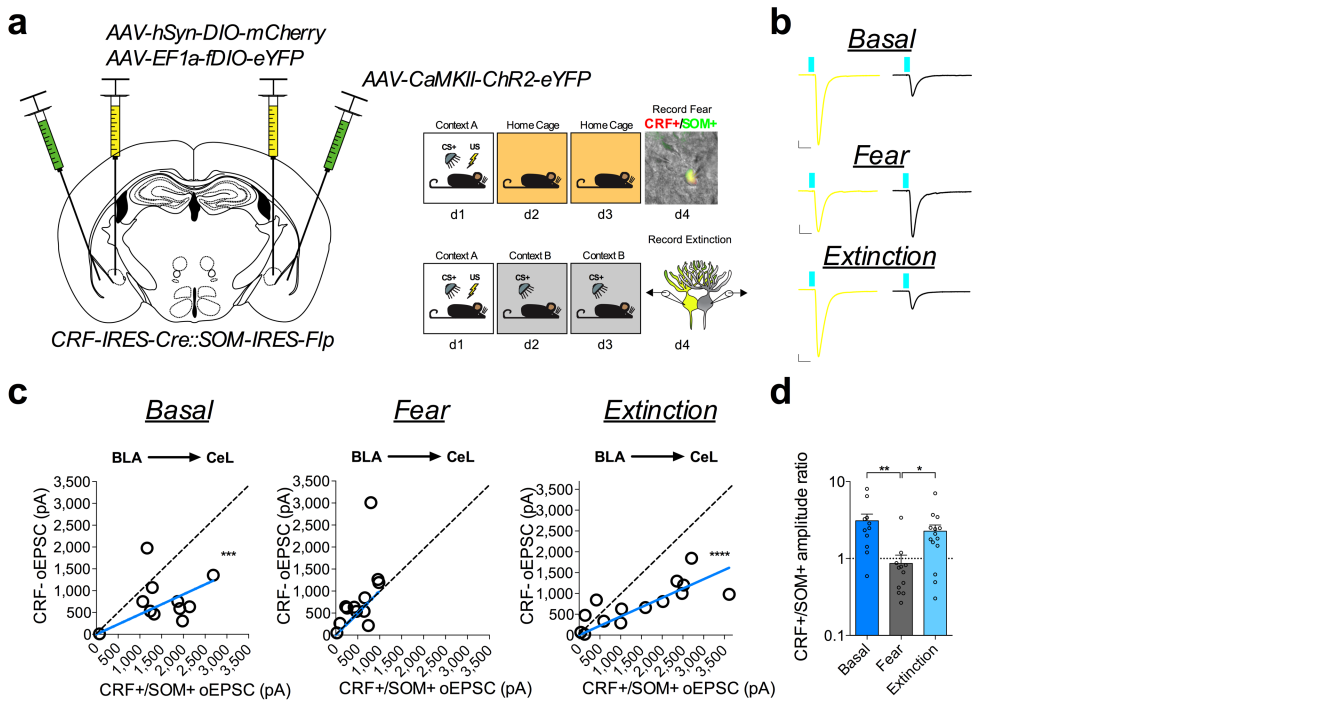

Supplementary Fig. 5. CRF+/SOM+ neurons demonstrate plasticity associated with CRF+ neurons. a, Left: optogenetic circuit mapping approach with viral injection. Right: experimental paradigm for dual patch-clamp recordings from CRF+/SOM+ (mCherry+/YFP+) neurons and adjacent CRF- neurons in fear conditioned and fear extinguished mice. Bottom-right: DIC and fluorescent overlay image of dual-patch clamp recording from CRF+/SOM+ and CRF- pair. **b,** Traces of maximal oEPSC amplitude from CRF+/SOM+ (yellow) and CRF- (black) neuronal pairs across behavioral conditions for stimulation of the BLA-CeL circuit (scale bars 10ms, 200pA basal, 10ms, 100pA fear, 10ms, 400pA extinction). **c,** XY graphs depicting skew-plot of maximal oEPSC amplitude from each CRF+/SOM+ and CRF- neuronal pair for behavioral conditions (n=11 basal pairs, 4 mice, n=12 fear pairs, 4 mice, and n=14 extinction pairs, 5 mice; extra sum-of-squares F test, $F_{(1,10)}$=29.83, P=0.0003 for basal, and $F_{(1,13)}$=121.0, P<0.0001 for extinction). **d,** Representation of CRF+/SOM+ and CRF- maximal oEPSC amplitude ratio (log scale; n=11 basal pairs, n=12 fear pairs, and n=14 extinction pairs; Kruskal-Wallis test, P=0.0026; post-hoc Dunn's multiple comparisons, basal vs. fear P=0.0022, fear vs. extinction P=0.0185). XY skew-plots are presented as absolute value. Bar graphs are presented as mean + S.E.M. *P<0.05, **P<0.01, ***P<0.001, ****P<0.0001.

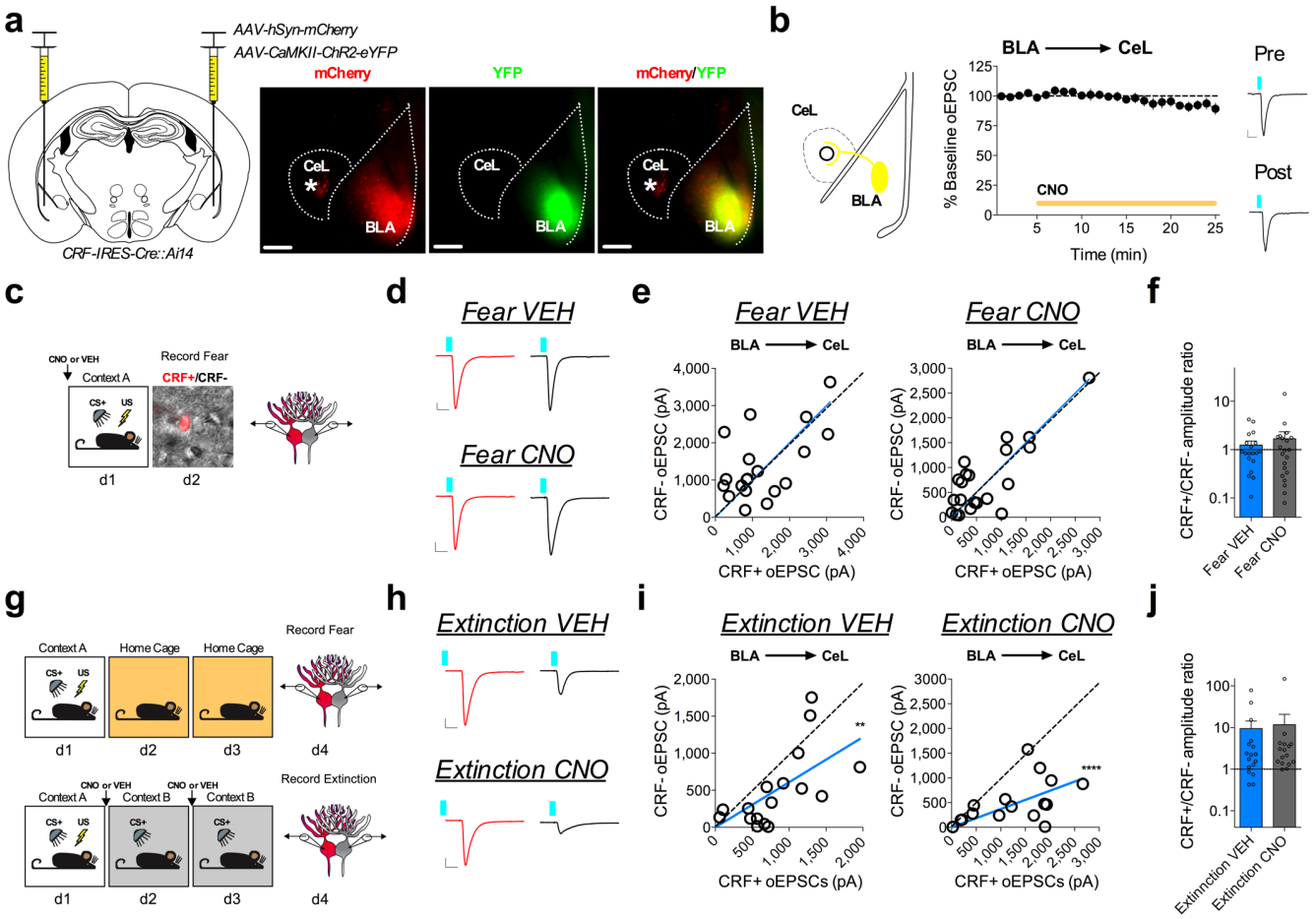

Supplementary Fig. 6. CNO administration does not affect plasticity in the BLA-CeL circuit. a, Left: mixed viral injection strategy for electrophysiological assessment of the BLA-CeL circuit in mCherry control animals. Right: image of ChR2-eYFP and mCherry expression in the BLA from a coronal slice used for recordings (*indicates CRF+ neurons in the CeL expressing TdTomato; scale bars 200µm); viral expression strategy was independently verified and repeated in *n*=3 mice. **b,** Left: schematic of ChR2-eYFP and mCherry co-expression in the BLA-CeL circuit. Right: summary data from bath application of CNO while recording oEPSC amplitude in the CeL (*n*=12 cells, 5 mice). Right: traces of oEPSCs before and after bath application of CNO (scale bar 10ms, and 200pA). **c,** Experimental paradigm of electrophysiological assessment of BLA-CeL circuit in mCherry control animals after fear learning. Bottom-right: DIC and fluorescent overlay image of dual-patch clamp recording from CRF+ and CRF- pair. **d,** Traces of maximal oEPSC amplitude from CRF+ (red) and CRF- (black) neuronal pairs across fear treatment groups for stimulation of the BLA-CeL circuit (scale bars 10ms, and 200pA). **e,** XY graphs depicting skew-plot of maximal oEPSC amplitude from each CRF+ and CRF- neuronal pair for behavioral conditions (*n*=19 fear VEH pairs, 5 mice, *n*=21 fear CNO pairs, 5 mice). **f,** Representation of CRF+/CRF- maximal oEPSC amplitude ratio (log scale; *n*=19 fear VEH pairs, *n*=21 fear CNO pairs). **g,** Experimental paradigm of electrophysiological assessment of BLA-CeL circuit in mCherry control animals after extinction training. **h,** Traces of maximal oEPSC amplitude from CRF+ (red) and CRF- (black) neuronal pairs across extinction treatment groups for stimulation of the BLA-CeL circuit (scale bars 10ms, and 200pA). **i,** XY graphs depicting skew-plot of maximal oEPSC amplitude from each CRF+ and CRF- neuronal pair for behavioral conditions (*n*=17

extinction VEH pairs, 4 mice, and n=16 extinction CNO pairs, 4 mice; extra sum-of-squares F tests for extinction VEH, $F_{(1,16)}$=15.43, P=0.0012, and extinction CNO, $F_{(1,15)}$=92.60, P<0.0001). **j,** CRF+/CRF- maximal oEPSC amplitude ratio (log scale; n=17 extinction VEH pairs, n=16 extinction CNO pairs). XY skew-plots are presented as absolute value. Bar graphs are presented as mean + S.E.M. **P<0.01, ****P<0.0001.

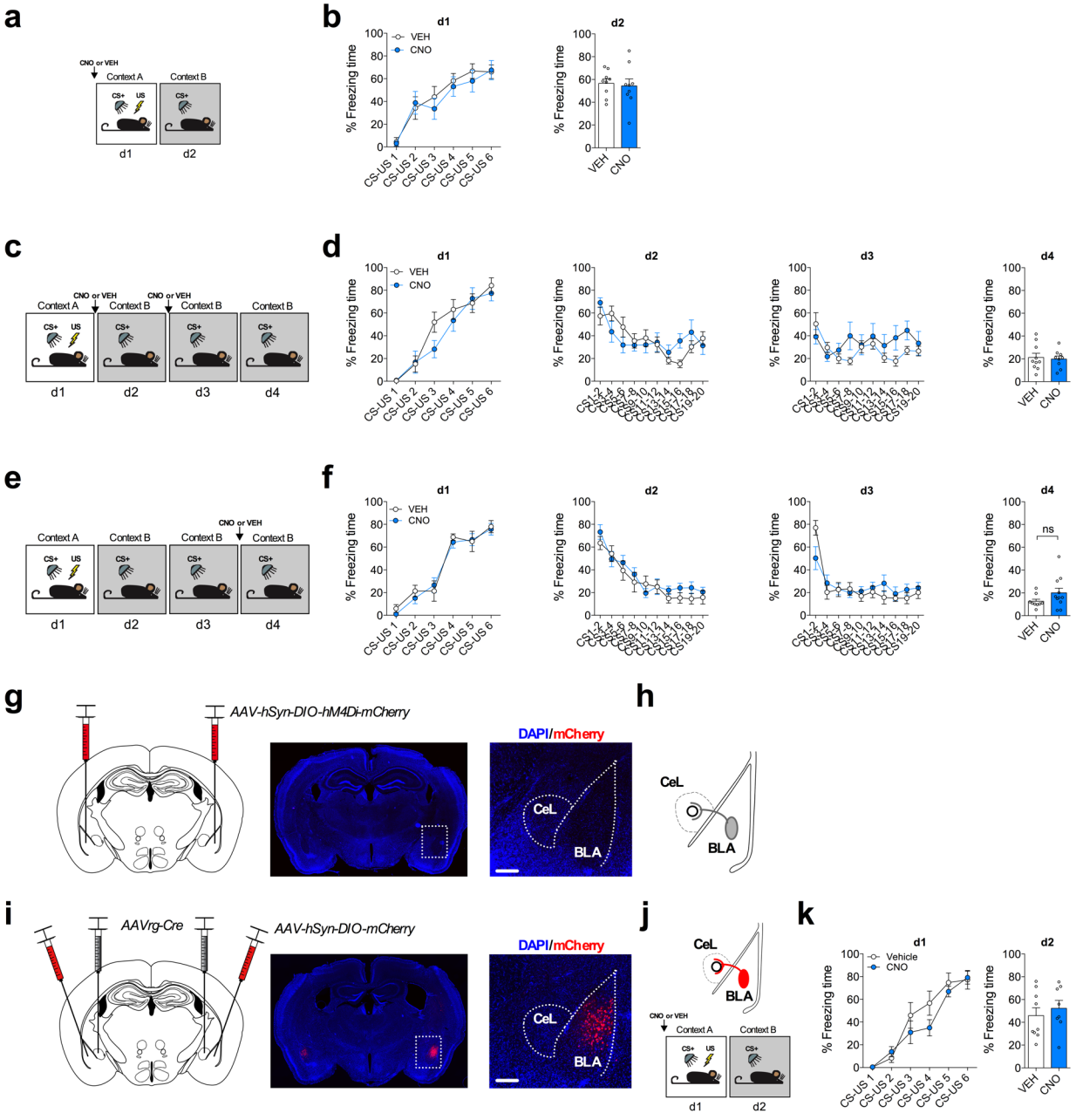

Supplementary Fig. 7. CNO administration does not affect freezing behavior. a, Experimental paradigm for administration of VEH or CNO during fear conditioning. **b,** Learning curves for VEH and CNO treated mice. Left to right, fear conditioning day 1 (d1), and fear memory recall test day 2 (d2) (*n*=9 mice per group). **c,** Experimental paradigm for administration of VEH or CNO during extinction learning. **d,** Learning curves for VEH and CNO treated mice. Left to right, conditioning day 1 (d1), extinction session 1 on day 2 (d2), extinction session 2 on day 3 (d3), and extinction memory recall test on day 4 (d4) (*n*=10 VEH mice, and *n*=9 CNO mice). **e,** Experimental paradigm for administration of VEH or CNO during an extinction memory recall test. **f,** Learning curves for VEH and CNO treated mice. Left to right, conditioning day 1 (d1), extinction session 1 on day 2 (d2), extinction session 2 on day 3 (d3), and extinction memory recall test on day 4 (d4) (*n*=9 VEH mice, and *n*=11 CNO mice; d4 two-tailed t-test, ns=non-significant, $t_{(18)}$=1.520, *P*=0.1458). **g,** Left: lack of intersectional injection

strategy for delivery of cre-dependent hM4D(Gi)-mCherry to the BLA. Right: images depicting absence of hM4D(Gi)-mCherry expression in the BLA when AAVrg-Cre is not injected into the CeA (scale bar 200μm); lack of viral expression was independently verified and repeated in *n*=3 mice. **h,** Schematic of lack of hM4D(Gi)-mCherry expression specifically in BLA neurons projecting to the CeL when AAVrg-Cre is not injected into the CeA. **i,** Left: intersectional viral strategy for behavioral assessment of control fluorophore expression in the BLA-CeL circuit. Right: images depicting bilateral expression of cre-dependent mCherry in the BLA with close up of inset (scale bar 200μm); viral expression strategy was independently verified and repeated in *n*=3 mice. **j,** Experimental paradigm for administration of VEH or CNO during fear conditioning. Top: schematic of mCherry expression specifically in BLA neurons projecting to the CeL. **k,** Learning curves for VEH and CNO treated mice. Left to right, fear conditioning day 1 (d1), and fear memory recall test day 2 (d2) (*n*=9 VEH mice, and *n*=8 CNO mice). Learning curves are presented as mean ± S.E.M., and bar graphs are presented as mean + S.E.M.

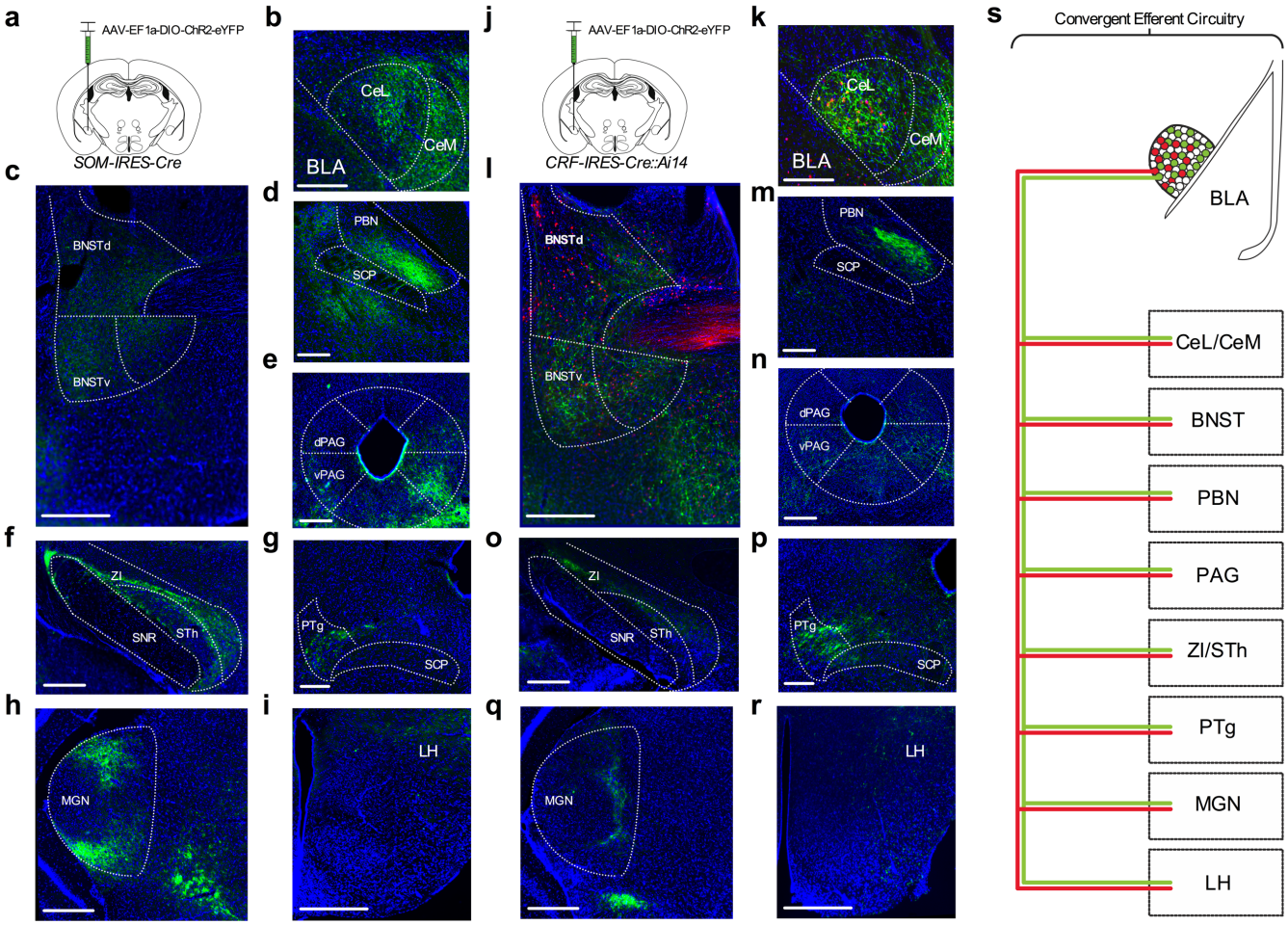

Supplementary Fig. 8. Convergent efferent projections of SOM and CRF neurons from the CeA. **a,** Optogenetic output circuit-mapping approach for Cre-dependent expression of ChR2-eYFP in SOM+ neurons of the CeA (*n*=5 mice). **b,** Local ChR2-eYFP cell body and synaptic terminal expression from SOM+ neurons in the CeL (scale bar 300µm). **c,** ChR2-eYFP synaptic terminal expression from SOM+ neurons in the dorsal and ventral BNST (scale bar 500µm). **d,** ChR2-eYFP synaptic terminal expression from SOM+ neurons in the PBN (note distribution of YFP in ventrolateral border of PBN; scale bar 200µm). **e,** ChR2-eYFP synaptic terminal expression from SOM+ neurons in the PAG (note distribution of YFP in the ventral and dorsal PAG; scale bar 400µm). **f,** ChR2-eYFP synaptic terminal expression from SOM+ neurons in the zona incerta/subthalamic nucleus (ZI/STh; scale bar 250µm). **g,** ChR2-eYFP synaptic terminal expression from SOM+ neurons in the pedunculotegmental nucleus (PTg; scale bar 250µm). **h,** ChR2-eYFP synaptic terminal expression from SOM+ neurons in the medial geniculate nucleus (note distribution of YFP in the dorsal and ventral MGN; scale bar 375µm). **i,** ChR2-eYFP synaptic terminal expression from SOM+ neurons in the lateral hypothalamus (LH; scale bar 500µm). **j,** Optogenetic output circuit-mapping approach for Cre-dependent expression of ChR2-eYFP in CRF+ neurons of the CeA (*n*=8 mice). **k,** Local ChR2-eYFP cell body and synaptic terminal expression from CRF+ neurons in the CeL (scale bar 300µm). **l,** ChR2-eYFP synaptic terminal expression from CRF+ neurons in the dorsal and ventral BNST (scale bar 400µm). **m,** ChR2-eYFP synaptic terminal expression from CRF+ neurons in the PBN (note distribution of YFP in dorsolateral border of PBN; scale bar 500µm). **n,** ChR2-eYFP synaptic terminal expression from CRF+ neurons in the PAG (note transient distribution of YFP in the ventral PAG relative to the dorsal PAG; scale bar 400µm). **o,** ChR2-eYFP

synaptic terminal expression from CRF+ neurons in the ZI/STh (scale bar 250μm). **p,** ChR2-eYFP synaptic terminal expression from CRF+ neurons in the PTg (scale bar 250μm). **q,** ChR2-eYFP synaptic terminal expression from CRF+ neurons in the MGN (note distribution of YFP in the medial MGN; scale bar 375μm). **r,** ChR2-eYFP synaptic terminal expression from CRF+ neurons in the LH (scale bar 500μm). **s,** Summary of convergent output structures of SOM+ and CRF+ neurons of the CeA.

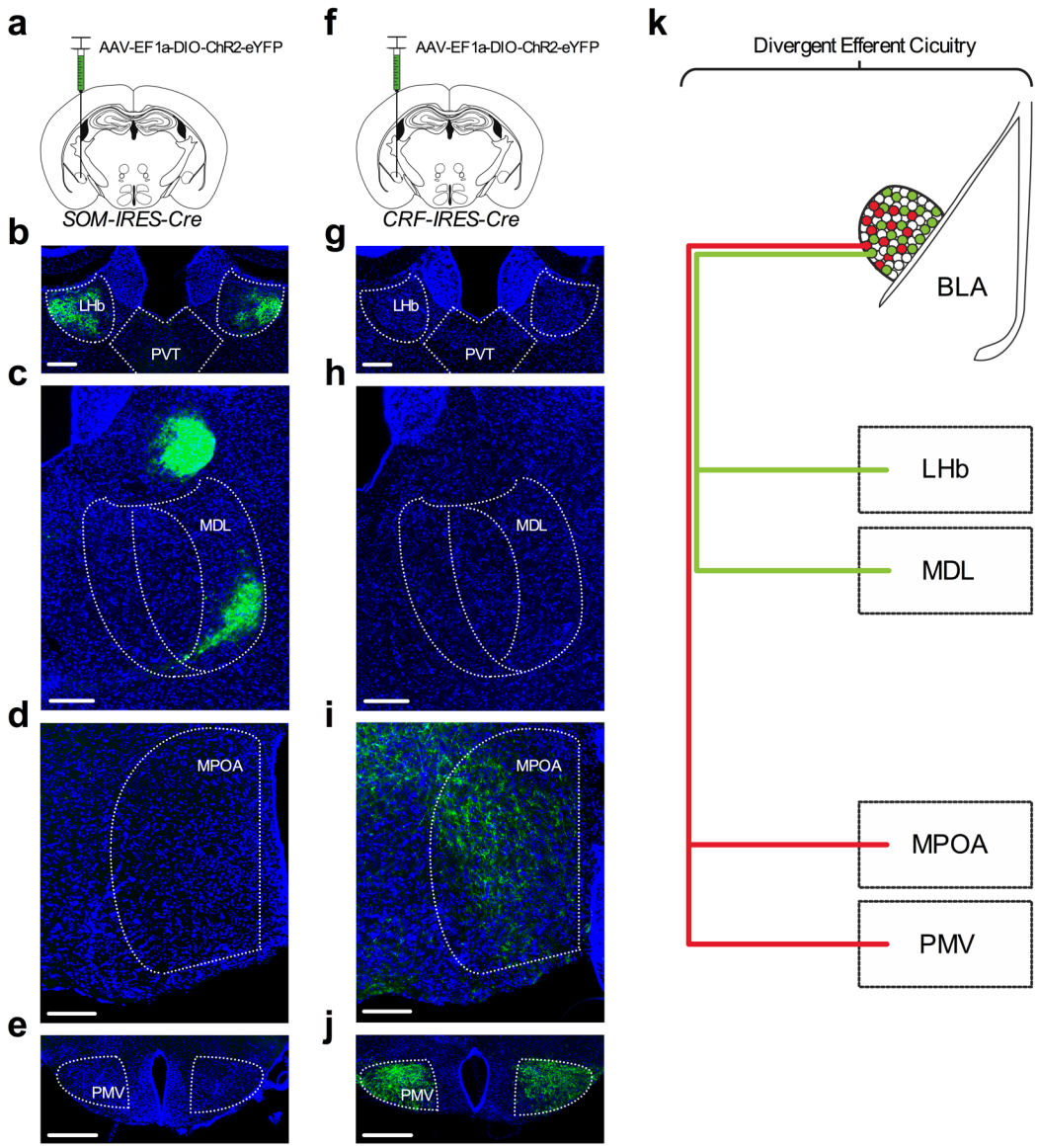

Supplementary Fig. 9. Divergent efferent projections of SOM and CRF neurons from the CeA. a, Optogenetic output circuit-mapping approach for Cre-dependent expression of ChR2-eYFP in SOM+ neurons of the CeA (*n*=3 mice). **b,** ChR2-eYFP synaptic terminal expression from SOM+ neurons in the lateral habenula (LHb; scale bar 250µm). **c,** ChR2-eYFP synaptic terminal expression from SOM+ neurons in the lateral portion of the medial dorsal thalamus (MDL; scale bar 125µm). **d,** Lack of ChR2-eYFP synaptic terminal expression from SOM+ neurons in the medial preoptic area (MPOA; scale bar 250µm). **e,** Lack of ChR2-eYFP synaptic terminal expression from SOM+ neurons in the ventral premammillary nucleus (PMV; scale bar 400µm). **f,** Optogenetic output circuit-mapping approach for Cre-dependent expression of ChR2-eYFP in CRF+ neurons of the CeA (*n*=3 mice). **g,** Lack of ChR2-eYFP synaptic terminal expression from CRF+ neurons in the LHb. **h,** Lack of ChR2-eYFP synaptic terminal expression from CRF+ neurons in the MDL. **i,** ChR2-eYFP synaptic terminal expression from CRF+ neurons in the MPOA (scale bar 250µm). **j,** ChR2-eYFP synaptic terminal expression from CRF+ neurons in the PMV (scale bar 400µm).

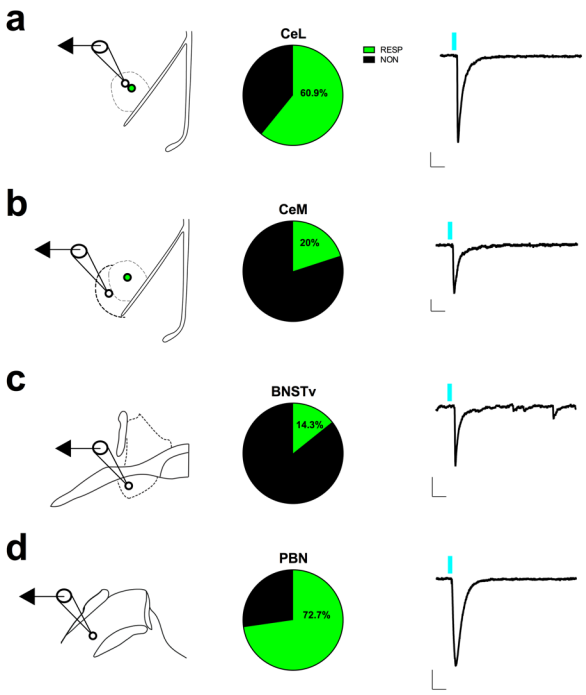

Supplementary Fig. 10. Connectivity index of CeA CRF+ neurons to areas with high or low ChR2-YFP terminal density. a-d, Percentage of responsive neurons from patch-clamp recordings of areas expressing visible YFP signal in slice (*n*=46 CeL, 7 mice, *n*=5 CeM, 3 mice, *n*=7 vBNST, 5 mice, and *n*=11 PBN cells, 2 mice; RESP=responsive, NON=non-responsive). Right column: representative traces of oIPSCs from responsive neurons in the CeL, CeM, vBNST, and PBN (scale bars 50ms, 100pA).

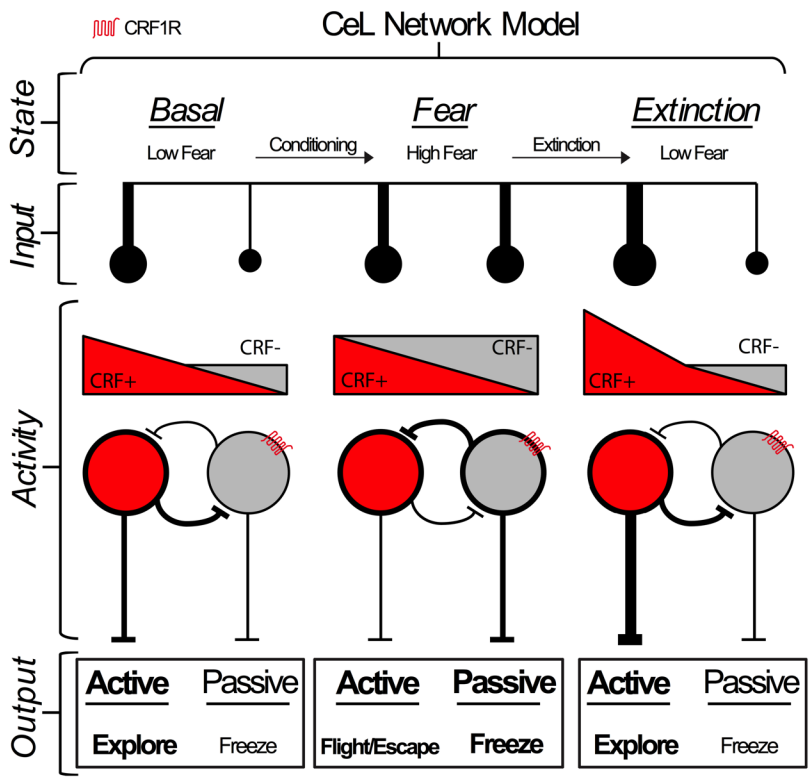

Supplementary Fig. 11. Summary of dynamic experience-dependent remodeling of CeL neuronal activity on the expression of fear behavior. This tiered CeL network model reflects overall input bias onto CRF+ and CRF- neurons across contextual states, the hypothesized activity of CeL neurons during excitatory drive from input sources, and the expected behavioral outputs. Since there is greater input onto CRF+ neurons in basal conditions, it is possible that salient sensory cues from the environment serve to drive active motivational states, such as exploration and foraging, behaviors that would require suppressing motor inhibition and are consistent with CeA-CRF+ neurons contributing to the expression of appetitive behavior under non-threatening contexts[16]. Previous findings suggest that during early or weak threat assessment, when association between stimuli and danger is still ambiguous, CRF+ neurons are recruited to selectively enhance associative learning through CRF release and subsequent CRFR1-mediated synaptic plasticity onto CeL neurons[13], which we further show results in equal relative sensory input from the BLA onto CRF+ and CRF-/SOM+ neurons. Following re-exposure to a threat-predictive CS, an animal can mount conditioned active or passive fear responses via mutually inhibitory connections between CRF+ and CRF-/SOM+ neurons, a result that reflects the predicted imminence or proximity of a threat and can be learned during extended training paradigms[2]. However, we propose that as the contingency between the CS and US degrades during extinction learning, such that the CS no longer accurately predicts threat exposure, there is a restoration of greater relative sensory input back onto CRF+ neurons, resulting in the suppression of passive freezing and the promotion of active exploration of the environment. This model is consistent with the overall role of CeA neurons impinging on hindbrain effector nuclei that tightly regulate motivational motor programs critical to survival[38,39].